Sediment Dynamics of a Divergent Bay–Marsh Complex

Daniel J. Nowacki[1] · Neil K. Ganju[2]

Abstract

Bay–marsh systems, composed of an embayment surrounded by fringing marsh incised by tidal channels, are widely distributed coastal environments. External sediment availability, marsh-edge erosion, and sea-level rise acting on such bay–marsh complexes may drive diverse sediment-flux regimes. These factors reinforce the ephemeral and dynamic nature of fringing marshes: material released by marsh-edge erosion becomes part of a bay–marsh exchange that fuels the geomorphic evolution of the coupled system. The dynamics of this sediment exchange determine the balance among seaward export, deposition on the embayment seabed, flux into tidal channels, and import to the marsh platform. In this work, we investigate the sediment dynamics of a transgressive bay–marsh complex and link them to larger-scale considerations of its geomorphic trajectory. Grand Bay, Alabama/Mississippi, is a shallow microtidal embayment surrounded by salt marshes with lateral erosion rates of up to 5 m year^{-1}. We collected 6 months of oceanographic data at four moorings within Grand Bay and its tidal channels to assess hydrographic conditions and net sediment-flux patterns and augmented the observations with numerical modeling. The observations imply a divergent sedimentary system in which a majority of the suspended sediment is exported seaward, while a smaller fraction is imported landward via tidal channels, assisting in vertical marsh-plain accumulation, maintenance of channel and intertidal-flat morphologies, and landward transgression. These results describe a dynamic system that is responsive to episodic atmospheric forcing in the absence of a strong tidal signal and the presence of severe lateral marsh loss.

Keywords Salt marsh · Geomorphic trajectory · Sediment flux

Introduction

A common setting in coastal environments is the coupled bay–marsh complex, which can be found along low-energy coasts, in microtidal and macrotidal regimes, both temperate and high-latitude settings (Allen and Pye 1992), and often near large sediment sources such as rivers (Fagherazzi et al. 2012). Embayments surrounded by fringing marsh incised by tidal channels form ephemeral systems (Fagherazzi 2013) whose components undergo joint geomorphic evolution as dictated by external and internal forcing mechanisms. Despite an acknowledgement of the importance of such environments, efforts to protect and restore bay–marsh complexes are typically hampered by a lack of knowledge regarding the overall sediment budget of the coupled system. These complexes are subject to physical forcing mechanisms such as sediment deficits from limited external sources, edge erosion from wave attack, and drowning from rising sea levels, three interrelated factors which determine in large part the geomorphic trajectory of bay–marsh systems.

Bay–marsh complexes are highly sensitive to external sediment availability, and proximity to such a source is a key factor driving the maintenance or expansion of a marsh system (Friedrichs and Perry 2001). External sediment availability is important both for vertical sediment accumulation on the marsh plain (e.g., Allen 2000; Friedrichs and Perry 2001), as well as the geomorphic maintenance of the overall coupled environment (e.g., Fagherazzi et al. 2012; Fagherazzi et al. 2013). Systems lacking a sufficient external sediment source will likely self-cannibalize and lose areal extent as a result.

Communicated by David K. Ralston

✉ Daniel J. Nowacki
 dnowacki@usgs.gov

[1] Pacific Coastal and Marine Science Center, U.S. Geological Survey, Santa Cruz, CA 95060, USA

[2] Woods Hole Coastal and Marine Science Center, U.S. Geological Survey, Woods Hole, MA 02543, USA

Marsh-edge erosion from waves serves to reduce the areal extent of a salt marsh, converting marsh to open-water embayment. This process is potentially the chief mechanism driving marsh loss worldwide (Marani et al. 2011), and the linear relationship between incident wave power and salt-marsh lateral erosion (Leonardi et al. 2016) indicates the sensitivity of marshes to the local wave climate. Storms that produce winds capable of generating large waves can raise water levels and drive episodic sediment deposition on the marsh surface (Reed 1989) and sediment import (Rosencranz et al. 2016), but they may also ultimately lead to sediment export (Ganju et al. 2013). A thorough review of storm impacts on salt-marsh dynamics and morphology is presented in Leonardi et al. (2018).

Sea-level rise can additionally modify the dynamics of a bay–marsh system. Assuming sufficient external sediment supply, accelerated rates of sea-level rise increase hydroperiod and subsequently deposition; without a sufficient sediment source, marsh drowning may result (Friedrichs and Perry 2001). Although sea-level rise may enhance marsh deposition, it can also drive erosion of tidal flats and marsh channels via stronger ebb currents, leading to sediment-flux divergence and a negative system-wide sediment budget (Zhang et al. 2020).

In this paper, we describe oceanographic observations, numerical wave model results, and relevant forcing mechanisms of sediment-transport dynamics within a bay–marsh complex. We compute the net sediment fluxes and illustrate the primary mechanisms via flux decomposition. These results are synthesized into a discussion of transgressive, divergent, barrier-free bay–marsh systems.

Study Area

Grand Bay is a subembayment of Mississippi Sound within the Gulf of Mexico, USA (Fig. 1). Straddling the Alabama–Mississippi border, it is located between the city of Pascagoula, MS to the west and Mobile Bay to the east. Along its shoreward boundary lie approximately 20 km^2 of salt marsh. Its seaward boundaries are the former Grand Batture Islands, now subaqueous shoals. Farther seaward lie Dauphin and Petit Bois Islands, which protect Mississippi Sound from swell propagating from the Gulf of Mexico. Much of the western side of the Grand Bay system is part of the Grand Bay National Estuarine Research Reserve (NERR).

Grand Bay is a diurnal microtidal system. It is also routinely subjected to daily sea breezes; these are strongest during April–August but can be present throughout the year. The weak daily tidal forcing combined with reliable daily winds can make discerning the influence of tides or winds challenging, because of the similarity of the relevant periods of these two distinct processes. This combination of frequent winds and weak astronomical tides can also lead

to seiche motions, which can vary the water level, flow velocity (e.g., Luettich et al. 2002), and biogeochemical processes (Basterretxea et al. 2011) in such environments.

The marshes of Grand Bay are composed of deltaic sediment delivered from the historical Escatawpa River, and Bayou Heron (Fig. 1) is thought to be one of its relict distributary channels (Eleuterius and Criss 1991). After an avulsion within the past 3000 years (Davies and Hummell 1994), the river today is a tributary to the Pascagoula River, which empties into Mississippi Sound at Pascagoula. The Pascagoula River is the closest riverine sediment source to Grand Bay, about 20 km west of the study site, and delivers about 8×10^5 t year^{-1} to Mississippi Sound. The Mississippi River, 150 km to the southwest, has a median sediment load of 1.3×10^8 t year^{-1} (Heimann et al. 2011). Because of the relative weakness of along-shelf flows near the mouth of the Mississippi, its sediment is generally not dispersed to far-afield areas (Wright and Nittrouer 1995) and its dynamics are likely not relevant to sediment transport within Grand Bay.

Over the past 300 years, numerous events have combined to increase available wave energy within Grand Bay. Barrier-island breaches and associated impacts from hurricanes in the 1700s and 1800s reduced the elevation of the Grand Batture Islands, which became severely fragmented by 1921 (Eleuterius and Criss 1991). By the 1950s, most of the Grand Battures had been reduced to subaqueous shoals, exposing the marsh shorelines of Grand Bay to greater wave energy. As a result, the marshes of Grand Bay experience extensive erosion from wave attack (Wacker and Criss 1996) at the fastest rates in the state of Mississippi (Mississippi Department of Marine Resources 1999). The 1848–2017 average lateral marsh erosion rate within Grand Bay, from the eastern side of South Rigolets Island to Point aux Pins (Fig. 1), is 0.53 ± 0.34 m year^{-1} (Terrano et al. 2019). Localized rates can be far higher: South Rigolets Island has experienced on average 4.5 m year^{-1} of erosion over the past 150 years (Meyer-Arendt and Kramer 1991). These rates, lower than modern values, still represent a considerable yearly sediment delivery to the system: Using an average Grand Bay marsh bulk density of 540 ± 240 kg m^{-3} (Morris et al. 2016; Marot et al. 2019), a 30-km perimeter around Grand Bay, a marsh height of 0.4 m (Ennis et al. 2013), and the Terrano et al. (2019) rate results in a yearly delivery of 3400 ± 2800 t of marsh material to Grand Bay. This delivery could be larger still given the potential for an effective marsh height relative to the bay bottom greater than 0.4 m (e.g., Wilson and Allison 2008). The large erosion rates are also manifested in the land-cover dynamics of Grand Bay NERR. The percent area of herbaceous wetland decreased from 56 to 50% between 1974 and 2001, with a nearly equivalent percentage increase in open water from 30 to 35% (Hilbert 2006).

Given the absence of other sediment sources in the vicinity of Grand Bay and the rapid rate of lateral erosion,
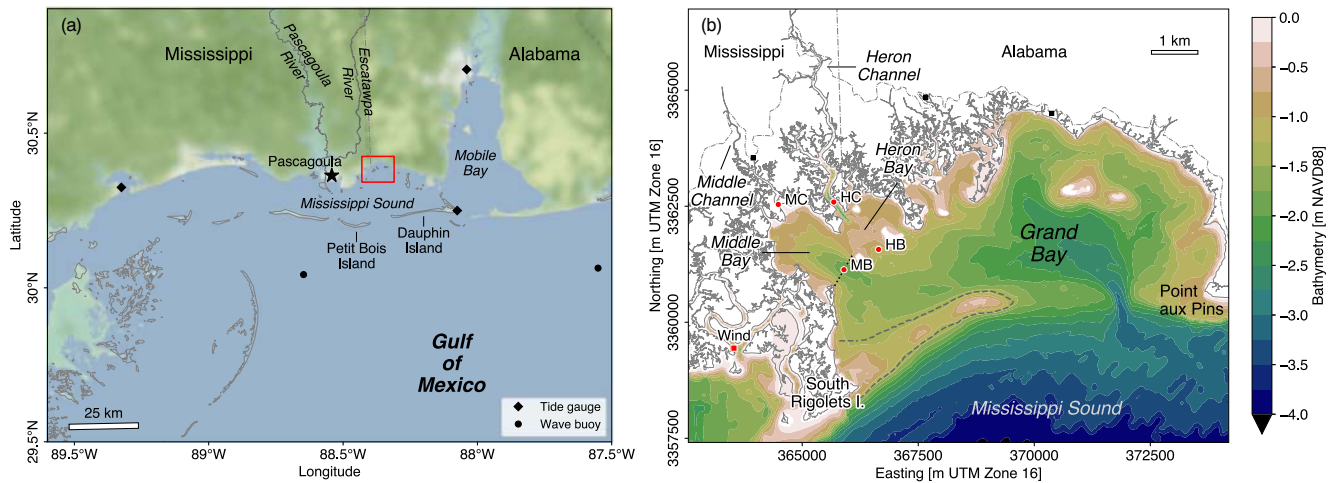
Fig. 1 a Map of US Gulf of Mexico coast and study area (red rectangle), NOAA tide gauges (diamonds), and NOAA wave buoys (circles). Background by Stamen Design, under CC BY 3.0; shorelines from GSHHG 2.3.7 (Wessel and Smith 1996). **b** Map of Grand Bay study area and instrument locations. "Wind" indicates Grand Bay NERR meteorological station. Dashed curve indicates approximate location of former Grand Batture islands. Dash-dotted line indicates marsh–upland boundary. Angled dotted line at MB is referenced in Fig. 3. Black squares are locations shown in Fig. 10. Bathymetry derived from DeWitt et al. (2017); shorelines from Terrano et al. (2019)

eroded salt-marsh material is likely an important source of sediment to the bay, but our knowledge of the ultimate fate of this sediment is limited. Is most conveyed upstream to help the marsh accrete and keep up with rising sea levels, or is it primarily lost offshore via ebb-dominant currents (Passeri et al. 2015)?

Methods

Field Deployment

Four oceanographic moorings were deployed in marsh channel–open bay pairs (Fig. 1). One pair characterized conditions in Heron Channel (HC) and its receiving basin Heron Bay (HB), while the other was deployed in Middle Channel (MC) and its receiving basin Middle Bay (MB). These two channel–bay pairs are adjacent drainages and subembayments of the Grand Bay system. Middle Bay (area 2.3 km^2) is larger than Heron Bay (0.67 km^2), but Middle Channel is smaller than Heron Channel. Middle Channel has a width of 50 m and is 3-m deep at the mooring and drains an area of 1.52 km^2, while Heron Channel is 140-m wide with a thalweg depth of 4 m and drains 4.51 km^2 of salt marsh. Both channels incise salt marsh predominantly colonized by *Juncus roemerianus* (Hilbert 2006), which is the predominant species of Alabama and Mississippi salt marshes (Eleuterius 1976).

Bottom-mounted instrument packages containing acoustic Doppler current profilers (ADCP; 2MHz Nortek Aquadopp Profiler), YSI EXO2 multi-parameter water-quality sondes, and RBR, Ltd. Virtuoso wave gauges were deployed at the four locations. Waves were measured every 30 min, and

all other parameters were measured every 15 min. Instruments were deployed from August 4, 2016, to January 26, 2017. New batteries were installed, and instruments were cleaned, downloaded, and redeployed on October 19–23, 2016, and no data are available from that period. Additionally, no data from the first deployment are available at HC. Measured data were subjected to established US Geological Survey quality-control procedures; further details are given in Nowacki et al. (2017). Turbidity measured 0.15 m above the seabed was converted to suspended-sediment concentration (SSC) using a repeated-median fit ($R^2 = 0.47$; Siegel 1982) following Suttles et al. (2019) and Nowacki and Ganju (2019). Auxiliary data including wind conditions and atmospheric pressure were obtained from the Grand Bay NERR meteorological station 3 km southwest of the study area (Fig. 1).

We computed water and sediment fluxes in the channels using cross-sectional ADCP measurements (Nowacki et al. 2018a) to convert the velocity measured in the channel thalweg to the channel-mean velocity and measured water level to channel cross-sectional area (Ruhl and Simpson 2005). In the bays, we used a bay-width computation to extrapolate measured currents and compute water and sediment flux; more details are given in the "Net Sediment Fluxes" section. In computing the sediment fluxes, we assumed a well-mixed vertical SSC distribution.

The measured sediment fluxes can be decomposed (e.g., Dyer 1974) into advective, dispersive, and Stokes components to determine dominant flux mechanisms.

$$F = \langle Q_t \rangle = \langle uaC \rangle = \underbrace{\langle \langle u \rangle \langle a \rangle \langle C \rangle \rangle}_{F_{adv}} + \underbrace{\langle u' \langle a \rangle C' \rangle}_{F_{disp}} + \underbrace{\langle u'a' \langle C \rangle \rangle}_{F_{stokes}}$$

$$+ \text{ small terms} \tag{1}$$

where u is the mean channel velocity, a is the channel area, C is SSC, angle brackets indicate tidally averaged values, and primes denote deviations from the tidal average. The first term on the right-hand side is the advective flux, arising from the subtidal terms, the second is the dispersive flux, attributable to the tidal-scale temporal correlation between velocity and SSC, and the third is the Stokes-drift flux, from the correlation between velocity and depth when tides are progressive; this term is zero for standing-wave tides. In this study, the Stokes term was negligible, and we focus on the advective and dispersive components.

Wave Modeling

In order to estimate the wave sheltering provided by the former Grand Batture islands and provide context for the modern-day geomorphic configuration and wave conditions, we implemented a numerical wave model of Grand Bay using SWAN version 41.31 (Booij et al. 1999). We ran SWAN in 2D stationary mode and specified a 0.75-m significant wave height at a 5-s period from 155°. These values are consistent with median statistics at NOAA buoys 42012 and 42067 (Fig. 1), although they likely represent an upper bound on waves propagating toward Grand Bay given the sheltering effects of Petit Bois and Dauphin Islands. We additionally specified a 10 m s^{-1} wind from the SE, simulating strong (99th percentile) onshore wind conditions. Model bathymetry was obtained from DeWitt et al. (2017) and the National Oceanographic and Atmospheric Administration Biloxi, Mississippi and Mobile Bay Coastal Digital Elevation Models. The model was run in two configurations: one using modern bathymetry and one representative of conditions when the Grand Batture islands were intact subaerial features. The islands were simulated in the model by introducing a line of dry cells without otherwise modifying the model bathymetry.

Results

Water Level, Velocity, and SSC

Tides are small in Grand Bay, with a maximum spring-tide range of about 1 m; neap tides range from 10 to 20 cm (Fig. 2a). This weak tidal forcing enables other influences on hydrodynamic conditions, particularly atmospheric pressure and wind, to dominate.

Flow velocities in channels are moderate (Fig. 2b), with maximum spring-tide currents approaching 0.4 m s^{-1}, and reaching 0.2 m s^{-1} during neaps. Currents in the bays are slower, with maximum velocities reaching only 0.15–0.2 m s^{-1}; bay currents are also more strongly influenced by

direct wind forcing than in the channels. At all locations, the tidal wave is approximately standing, except for within the channels when water levels were within 30 cm of the salt-marsh elevation, when velocities increased by a factor of 2–3. These surges, caused by the geomorphic configuration of the channel within the tidal prism and flooding and draining of the marsh platform (e.g., Myrick and Leopold 1963; Pestrong 1965), were present on both floods and ebbs.

SSC characteristics in the channels and bays were distinct and were not correlated with Pascagoula River sediment discharge. In the Middle Bay–Middle Channel system, average bay SSC was about 50% greater than channel SSC. Average Heron Channel SSC was more comparable to Heron Bay SSC, likely because of the smaller area and resuspension potential of Heron Bay. Overall, mean SSC was 24 mg L^{-1}; 95% of the values fall between 6–75 mg L^{-1}.
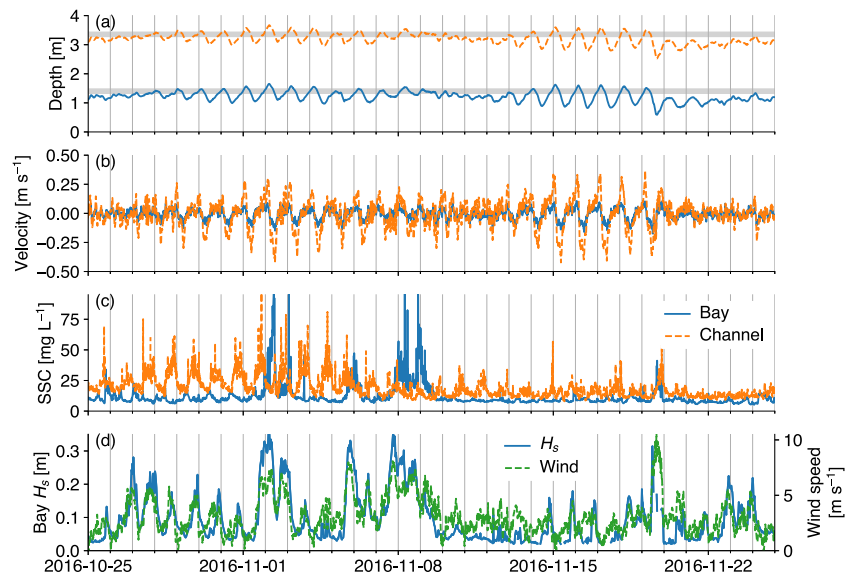
In the bays, there is little tidally forced SSC variability (Fig. 2c). Instead, most variation comes from wind events that generate waves capable of resuspending bed sediment and eroding the marsh edge. Bay SSC was generally higher on ebb tides than flood tides, suggesting a sediment-exporting environment. SSC in the channels varies over a range of time scales, including hourly, tidal, and storm scales, as SSC is transported from the bay as well as locations farther upstream. The tidal surges in the channels did not meaningfully alter the SSC. Velocities in the channels were ebb-dominant, but SSC tended to be greater on floods than ebbs. This flood–ebb SSC differential suggests a channel environment that fosters sediment import (Ganju et al. 2017; Nowacki and Ganju 2019) and may imply that channels serve to sequester sediment in the marsh and channel-adjacent flats.

Wind Influences

Two primary forms of wind forcing are active in Grand Bay. During the late summer and early fall, daily sea breezes from the SSE regularly occur and peak in mid afternoon. Average sea breezes are about 3 m s^{-1} but can peak to 6–8 m s^{-1}, speeds sufficient to generate moderate wind waves in the bays. A shift in the wind regime occurred in early November, when wind forcing changed from daily sea breezes to larger-scale frontal passage and stronger, more sustained wind events. Although diurnal sea breezes occur during the late fall and winter, their magnitude is reduced and larger storms become more important.

The transition from sea breezes to event-driven dynamics is visible in Fig. 2. Prior to 8 November, SSC is relatively high and results from consistent sea breezes eroding the marsh (U.S. Geological Survey 2017) and resuspending bed material. After this date, SSC is lower, because there is less wind and wave forcing within the bay and no larger events

Fig. 2 Time-series plot showing **a** water depth, **b** flow velocity, and **c** SSC at channel (HC) and bay (HB) locations, and **d** significant wave height at HB and wind speed at Grand Bay NERR meteorological station. Horizontal lines in (**a**) indicate approximate marsh level (Smith et al. 2020) relative to the channel and bay water depths

to impact the system. The bay and channel environments responded differently to wind forcing, and we consider them individually below.

Wind Influences on Bay Dynamics

Within bays, winds modify waves, water level, and currents. Wind-generated waves resuspend material on the bed and erode the marsh edge. Indeed, SSC in the bay is responsive to wind over a range of wind speeds, particularly during landward winds (Fig. 3a). Larger waves produced by stronger wind events can erode more bed material and deliver more energy to attack the marsh edge. Furthermore, landward winds have greater fetch and are able to produce larger waves which are more efficient in mobilizing sediment from the bed and marsh edge. These larger waves result in

higher SSC values at MB for landward winds compared to seaward winds.

In the semi-enclosed Heron and Middle Bays, wind modifies currents via direct application of stress to the water surface, as well as the production of water-level setup that drives a return flow in the deep regions of the bay (Csanady 1973; Signell et al. 1990; Wong 1994). This return flow is revealed in the sediment flux (Fig. 3b). Landward winds produce seaward sediment fluxes at MB, and the magnitude of these fluxes increase with wind speed. Seaward winds with a strong southward component consistently produce landward sediment fluxes that are aligned with the local bay isobaths. Seaward winds with a weaker southward component result in more variable sediment-flux directions, potentially because of the sheltering effect of the island which separates Middle and Heron Bays.
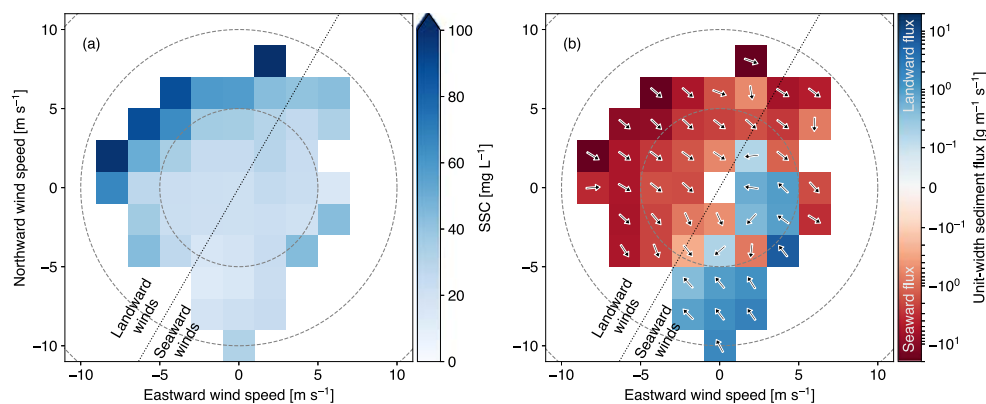

Fig. 3 Plots of mean **a** SSC and **b** sediment flux at MB binned by wind conditions with arrows indicating flux direction. Bins are plotted only if they include 20 or more data points. Circles indicate 5 m s^{-1} speed increments. Angled dotted line indicates orientation normal to axis of Middle Bay (see "Introduction"); wind conditions above this

line correspond to landward winds. In (**a**), note increase in SSC with strong landward winds. In (**b**), note seaward sediment flux for landward winds and variable but generally landward flux during strong seaward winds

Wind Influences on Channel Dynamics

Wind speed does not exhibit a clear correlation with SSC in channels as it does in bays. Instead, the wind–SSC correlation is more subtle, but no less crucial, to the sediment dynamics. Wind influence in the channels is primarily manifested in the form of seiche motions. Seiches are a key effect of both storms and sea breezes in channels, and are typically produced by a sudden change in wind characteristics, such as a directional change, an increase in wind speed, or a rapid decrease in winds. Water-level variability, flow velocity, and sediment fluxes are all influenced by seiche activity, which takes on increased importance in this microtidal environment. The combination of high SSC in the bay and seiche motions in the channel is a method by which considerable sediment is transported within channels.

Although the specific wind dynamics leading to each seiche event varied, we consider one example to elucidate typical patterns. In early January 2017, variability in wind forcing produced seiche motions at HC (Fig. 4). Moderately strong winds blew westward and transitioned to northward at about 5 m s^{-1}, building bay waves to significant heights of 0.2–0.3 m. Concurrently, bay SSC increased. As the wind relaxed, the release of water-level setup initiated several actions in rapid succession.

Water-level drawdown in the bay started a strong ebbing seiche motion in the channel (denoted by "1" in Fig. 4). Channel flows nearing 0.5 m s^{-1} resuspended sediment which potentially had settled on the bed over the preceding 8 h of weak currents. During this ebb-directed seiche, material was transported seaward out of the channels. A flood seiche (2) brought water and moderate amounts of sediment back

into the channels. During the next ebb seiche (3), SSC in the bays increased, and on the following flood seiche (4), channel SSC markedly increased, as this high-SSC water was transported back into the channel. Motions continued (5, 6, 7, 8) for another 4 h. The pattern of increased fluxes of water and sediment for this event occurred over about 8 h, with a seiche period of about 2 h.

For an open basin, the period T of the fundamental seiche mode is (e.g., Gill 1982):

$$T = \frac{4L}{\sqrt{gh}} \quad (2)$$

where L is a horizontal length scale, g is gravity, and h is a vertical length scale. Representative values of 4–6 km for L and 1–1.5 m for h give T values of 1.15–2 h. As such, the seiche periods plotted in Fig. 4 are consistent with Fig. 2.

We use a coherent wavelet transform (CWT) to visualize seiche influence on the velocity and sediment flux (Fig. 5), because seiches do not occur as consistently as astronomical tides, and the variability they produce can be subtle when considering the full deployment time-series. The velocity CWT shows a band of elevated energy at the diurnal tidal period and, to a lesser extent, the semidiurnal period. The energy in the tidal bands varies with the spring–neap cycle, and seiches can occur during both spring- and neap-tide periods, as shown in Fig. 5. At the seiche-period band, Fig. 5 shows at least three distinct seiche events in the velocity, on 1 January, 2–3 January (the event shown in Fig. 4), and 6–7 January. Similarly, the sediment-flux CWT shows increased energy in the seiche band, as well as at higher and lower periods.

The typical magnitude of seiche-induced velocities in the channel is 25–50 cm s^{-1}, greater than typical channel

Fig. 4 Seiche event on 2–3 January 2017 at Heron Bay and Heron Channel. **a** Wind vectors and significant wave height in Heron Bay. **b** SSC at the bay and channel locations. **c** Along-channel velocity (positive flood) and sediment fluxes (positive import). Numbers in (**c**) are referenced in the text
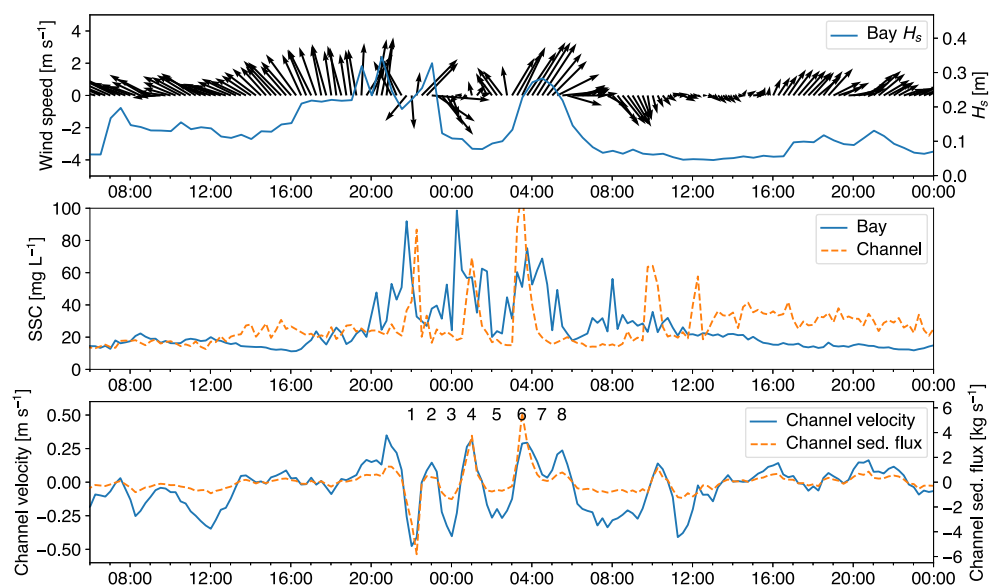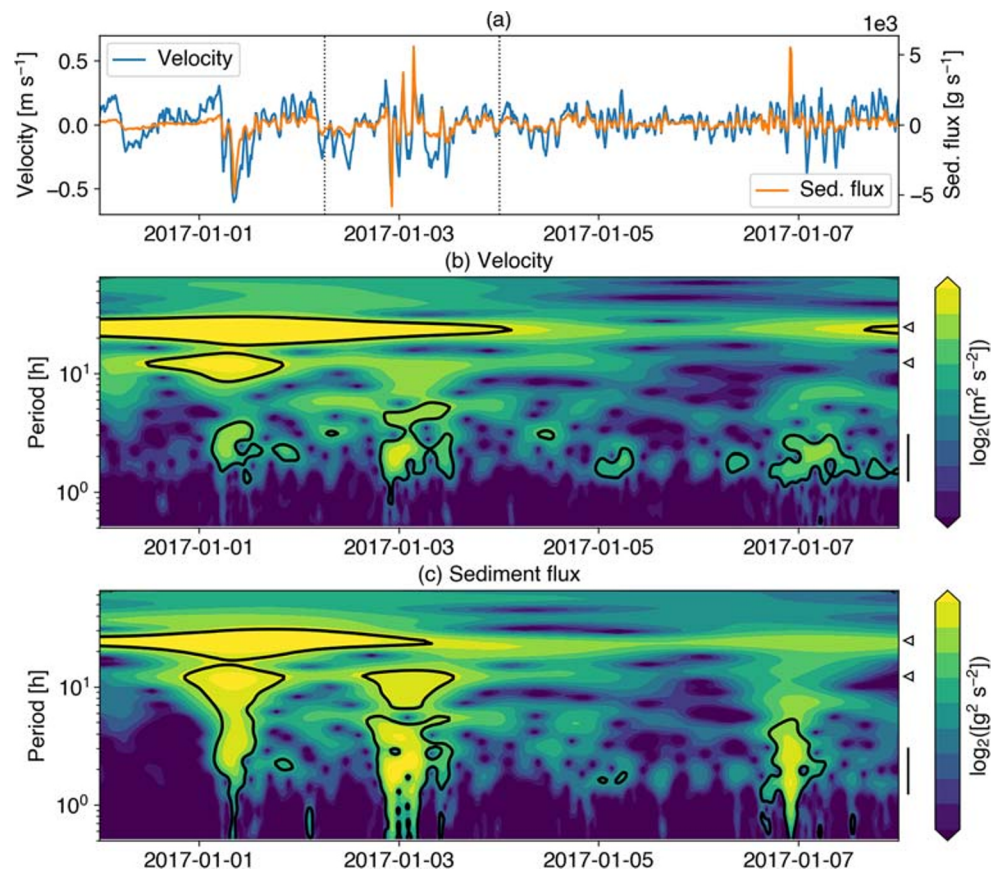
Fig. 5 **a** Time-series of velocity and sediment flux at HC in early January 2017. Vertical lines indicate extent of Fig. 4. **b** Continuous wavelet transform (CWT) of velocity computed using a Morlet mother wavelet. **c** CWT of sediment flux. Brighter colors indicate increased energy and black contours indicate the 95% significance level. Triangles at right of (**b**) and (**c**) indicate diurnal and semidiurnal tidal periods; vertical lines span periods of 1.25–3 h, the range of seiche motions that correspond to the dimensions of Grand Bay

tidal velocities of 20–40 cm s^{-1}. Using traditional Fourier-transform analysis averaged over the full deployment, 13–21% of the velocity energy and 17–25% of the sediment-flux energy in channels were in the seiche band, compared to 46–62% and 32–43% for the tidal band. During periods of considerable seiche activity in the channels (e.g., the time range of Fig. 5), the seiche band represented 33–35% of the velocity energy and 39–47% of the sediment-flux energy, compared to 24–33% and 14–19% in the tidal band.
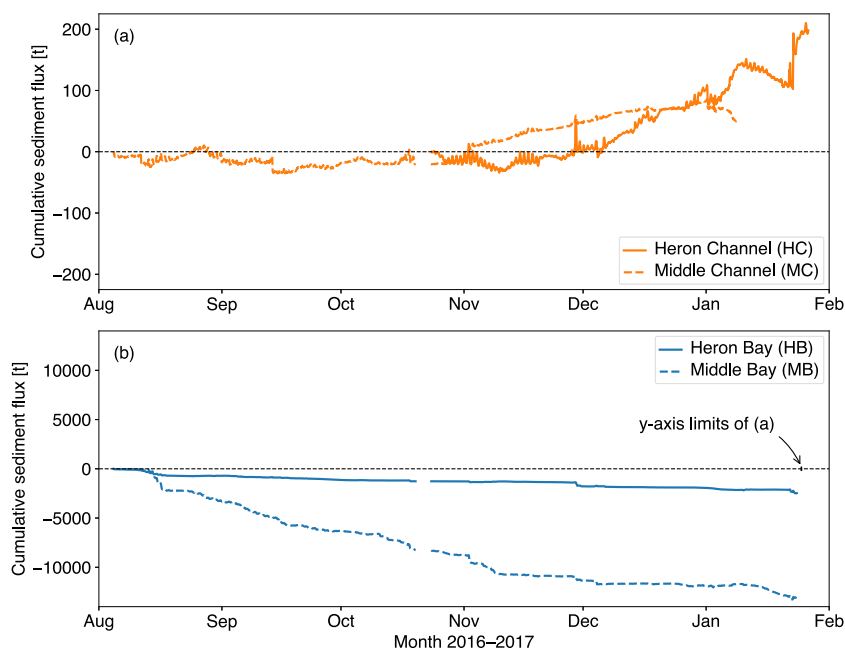
Net Sediment Fluxes

Channels

Over the 6-month deployment, channels were neutral to net importers of sediment (Fig. 6). Sediment was imported at MC at a rate of 120 t year^{-1}. During the shorter period available at HC, the import rate was equivalent to about 700 t year^{-1}; the lack of the more quiescent summer period at HC may lead to a biased value, rendering it not directly comparable to MC. The HC cumulative sediment flux shows evidence of the stronger tidal currents and seiche motions in Heron Channel, as well as its larger cross-sectional area. In contrast, at MC, a consistent landward trend in import is present for the majority of the deployment.

Comparing the summer and fall versus winter trends at MC suggests that stronger storms in the winter months increased the magnitude of sediment import in the channels. The elevated landward import rate beginning in early December was driven both by punctuated increases from seiche motions and a shift in the direction of the advective flux component (1) from neutral to landward (dispersive flux was consistently landward). The shift in flux direction could be caused by changes in river flow, evapotranspiration rate, or water-mass routing within the marsh interior. Using the range 120–700 t year^{-1} and the drainage areas of Heron and Middle Channels corresponds to an area-normalized channel import rate of 300 ± 40 t km^{-2} year^{-1}. (Because the field deployment did not capture a full year of observations, the annualized values reported here may not represent typical yearly conditions. Additional potential sediment import during unmeasured frontal passage in late winter and spring may render our reported values underestimates of the true net sediment import. Similarly, unmeasured calm periods would cause our values to overestimate the import rate.) During the period of concurrent deployment, net sediment fluxes at HC and MC were similar, despite a Middle Channel creekshed area that is only about 25% that of Heron Channel. One reason for this difference may be that Middle Bay is about 3.5 times larger than Heron Bay

Fig. 6 Cumulative sediment flux at **a** the channel sites and **b** the bay sites. No data from HC are available from the first deployment. Positive values indicate import and negative values indicate export. Channels are neutral to sediment importing, while bays consistently export

and provides a greater pool of available sediment via a larger marsh perimeter and seabed area. In this way, the larger bay area may compensate for the smaller channel in the Middle Bay–Channel system.

Events in mid August and September, as well as early November, December, and January, were typically seiche driven and resulted in both temporary import and export. Peaks in velocity, sometimes exceeding 0.8 m s^{-1}, efficiently flushed or imported sediment from the system over periods of 1–2 h. Indeed, channels often imported considerable sediment on the flooding seiche wave, only to be exported during the following phase of the seiche. After export events, gradual re-import of sediment occurred in the days following.

Over 1 year, the amount of material transported into (and out of) Heron and Middle Channels is of order 2500–5000 t, values similar to the 3400 ± 2800 t year^{-1} estimated to be delivered to Grand Bay from local marsh erosion. Taken together, these values suggest considerable recycling of material into and out of the channels before it is eventually sequestered on channel flanks or the marsh platform, or lost to seaward locations.

Bays

Although computing the sediment fluxes in the channels is relatively straightforward, the unconstrained geometry of the bays invites additional complexity. A naïve approach assumes that conditions at HB and MB are representative of conditions across the full width of those bays. Given the strong influence of wind on the flow dynamics and

the semi-enclosed nature of the bays, it is likely that there is seaward flow in the deep part of the channels (i.e., at the moorings) and landward flow in the shallows during frequent landward wind events. In this environment, assigning conditions as measured in the center of the bay to shallower edge regions ignores such landward flow along the flanks. The observed magnitude of seaward flux also could be inflated by landward flux of sediment from elsewhere in the greater Grand Bay system and recycled back out via the deeper portion of Middle Bay. Nevertheless, using the simple approach, Heron Bay exports about 5000 t year^{-1}, while Middle Bay exports about 30,000 t year^{-1}. When normalizing by the perimeter of each bay, these values become marginally more comparable, about 2 t m^{-1} year^{-1} at HB versus 5 t m^{-1} year^{-1} at MB.

The magnitude of net export nearly always increased during wind events in the bays. Such events occurred in mid August, mid September, early November, and early December (Fig. 6), and each was characterized by similar conditions. In general, moderate to strong winds from the southeast—the direction of maximum fetch—produced significant wave heights in the bays of order 0.3 m, often increasing SSC to more than 100 mg L^{-1}. Wind-driven circulation dynamics in the closed-ended Heron and Middle Bays resulted in net offshore velocities at the monitoring locations. The combination of increased SSC and offshore flow led to enhancement of the sediment export from the bays (Fig. 3b). The strong offshore flux occurring during these events may be partially balanced by onshore velocities at the shallow bay margins, as described in the "Wind Influences on Bay Dynamics" section.

Flux Decomposition

The decomposed fluxes (1) illustrate the contrasting sediment-transport processes active in the channels and bays. Weak tidal currents and subdued seiche velocities in the bays, which are the major components of the dispersive flux, result in minimal values for this term (Fig. 7). Instead, storm-scale advective processes—bed resuspension and marsh-edge erosion—are most important within the bays and dominated the decomposed fluxes. In other systems with a more dominant fluvial influence, the advective term would often be associated with changes in river forcing. Here, in this environment lacking a nearby river source, storm events are the most relevant advective process.

Considering the stronger tidal currents and seiche velocities in the channels compared to the bays, along with the tidally influenced SSC (Fig. 2), we might expect dispersive terms to be more dominant there. Indeed, the total channel sediment flux is roughly evenly distributed between the advective and dispersive terms. Although subtidal processes like storm events associated with frontal passage are relevant in channels, shorter-term processes including tidal flow and seiche motions are similarly important in transporting sediment within channels.

Modeled Wave Conditions

Modeled wave conditions within Middle and Heron Bays are dramatically different with and without the presence of the Grand Batture Islands. At representative locations within Middle and Heron Bays, wave heights increased 10–24% and wave periods increased 8–24% after loss of the intact subaerial Grand Batture islands (Fig. 8). The inability of the shoals to fully block waves allowed additional offshore swell to penetrate the shallow waters within Grand Bay. Wave power ($E \cdot c_g$) increased 34–109% at the representative locations. Along the marsh edge of Middle Bay, wave heights increased an average of 15% (Fig. 8 inset). We expect marsh erosion to have increased by a

concomitant rate with subaqueous Grand Battures given the linear relationship between wave power and marsh erosion (Marani et al. 2011; Leonardi et al. 2016). The increase in erosion liberates more material which, in theory, can be transported into the channels and onto the marsh platform to enable to marsh to accumulate sediment as it transgresses landward.

Discussion

Sediment Dynamics of a Barrier-Free, Divergent System

Salt marshes are ephemeral environments perpetually in flux (Fagherazzi 2013) and are a key element of the coupled bay–marsh complex. External forcing mechanisms such as sea-level rise, wave attack, and sea-level rise serve to modulate the marsh among states of erosion, equilibrium, and expansion. Barrier islands protect the back-barrier environment from offshore waves (Defne et al. 2020), and the loss of the barrier can result in increases of up to 700% in wave energy impacting the coast (Stone and McBride 1998). The modern Grand Bay system is responding to the loss of the Grand Batture islands with increased marsh erosion from wave attack. Observed lateral marsh erosion over the past century combined with seasonal-scale measurements of sediment fluxes in channels and bays lead to a conceptual model of sediment dynamics within Grand Bay (Fig. 9). Increased modern wave energy, formed by daily sea breezes and frontal storm passage (Fig. 2), erodes the marsh edge and creates a large pool of available sediment. Flux divergence leads to a duality of fates for this material: sediment export to the ocean as well as landward sediment import. A majority of the material eroded from Middle and Heron Bay is transported to points seaward (Fig. 6), and the rate of export at MB is several times greater than that at HB, reflecting the different sizes of the bays and amounts of available sediment in each. In a similar fashion, the larger

Fig. 7 Fractional flux decomposition showing advective (F_{adv}/F) and dispersive (F_{disp}/F) components at the **a** channel and **b** bay locations. Channel sites exhibit a mix of advective and dispersive forcing, while bays primarily are driven by advective processes
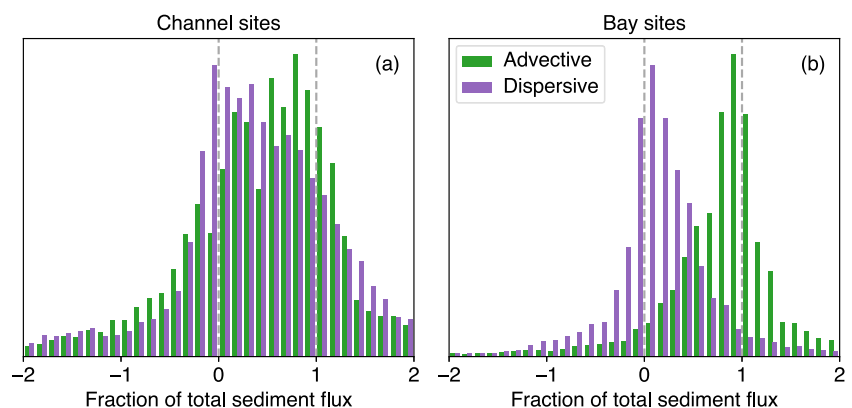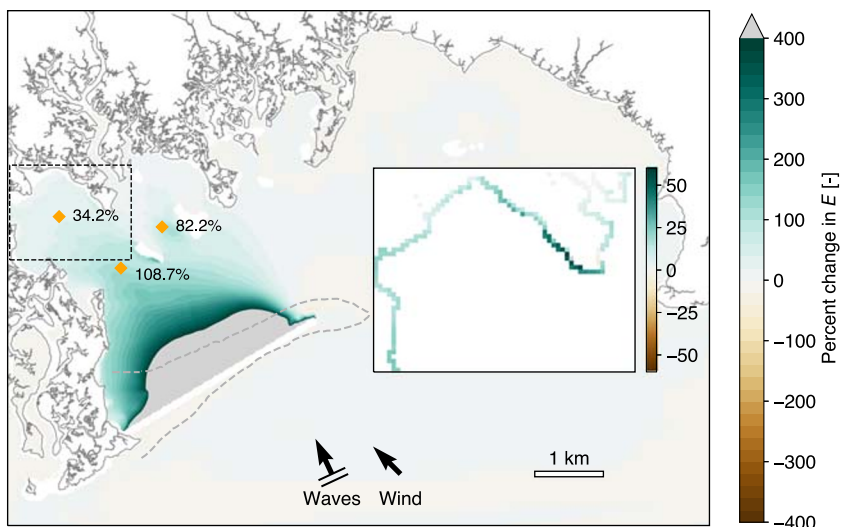
Fig. 8 Percent change in wave power without subaerial Grand Batture Islands. Marker labels indicate percent increase in wave power at selected locations in Heron and Middle Bays. Dashed curve indicates approximate location of former Grand Batture islands, implemented as a line of dry cells (angled white line) in the model. Inset shows edge cells from model domain in Middle Bay to emphasize change at the marsh edge; note change in colorbar limits

size of Heron Channel leads to greater landward transport at HC than at MC. The portion that is transported up channels is likely deposited on channel flanks and the marsh platform to assist in its landward transgression, bolstering the resilience of the system in an effort to prevent drowning (Mariotti and Carr 2014). These characteristics describe a divergent sedimentary system whose source is the marsh edge and whose sinks are the channel–marsh system and points seaward.
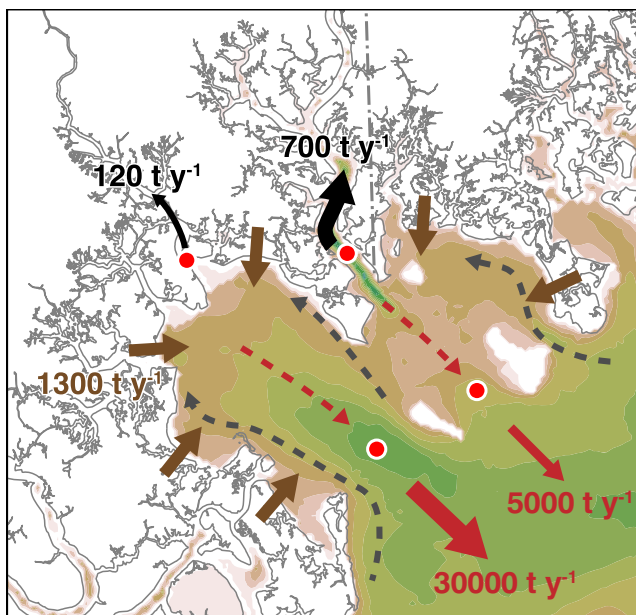

Fig. 9 Conceptual diagram of Middle and Heron Bays showing marsh erosion (brown arrows), sediment import to channels (black arrows), and sediment export to the ocean (red arrows). Dashed arrows indicate inferred wind-influenced flow velocity facilitating export in the deep portion of the bays. Circles indicate mooring locations

Just as the seaward edge of the marsh is eroding, the landward edge of the marsh appears to be transgressing. Visual comparison of aerial photos over a timespan of 26–27 years suggests landward migration of marsh vegetation to areas previously featuring upland characteristics (Fig. 10). Formerly unvegetated areas near tree islands were colonized by marsh vegetation (Fig. 10 left), and regions previously consisting of upland vegetation were degraded and replaced by marsh vegetation (Fig. 10 center and right). Figure 10 right additionally shows landward migration of the marsh shoreline. These changes indicate localized marsh–upland transgression of 10–30 m, equal to rates of 0.4–1.1 m year^{-1}. The computed values are of similar order to the marsh-edge erosion rates and prompt consideration of this system as one successfully migrating landward and not merely losing area at its seaward edge (e.g., Schieder et al. 2018). These visual comparisons suggest the feasibility of using remote sensing to assess the landward and seaward migration rates of the overall system.

FitzGerald et al. (2004) described a conceptual model of marsh decline in mixed-energy barrier-island chains that superficially resembles the dynamics of Grand Bay. In that model, increasing rates of sea-level rise lead to loss of barrier-island volume, changes in the tidal prism, and conversion of marsh to open water. Similarly, the loss of the Grand Batture islands has led to open-water conversion within Grand Bay at the seaward marsh edge. Our results suggest that the increased wave energy available from the loss of the Grand Battures (Fig. 8) is at least as important as sea-level rise in driving the marsh loss. Indeed, sea-level rise is not a requirement for marsh loss; without sufficient external sediment supply, marshes can retreat laterally via wave attack alone (Fagherazzi et al. 2013). Here we suggest an expansion of the FitzGerald et al. (2004) model in which
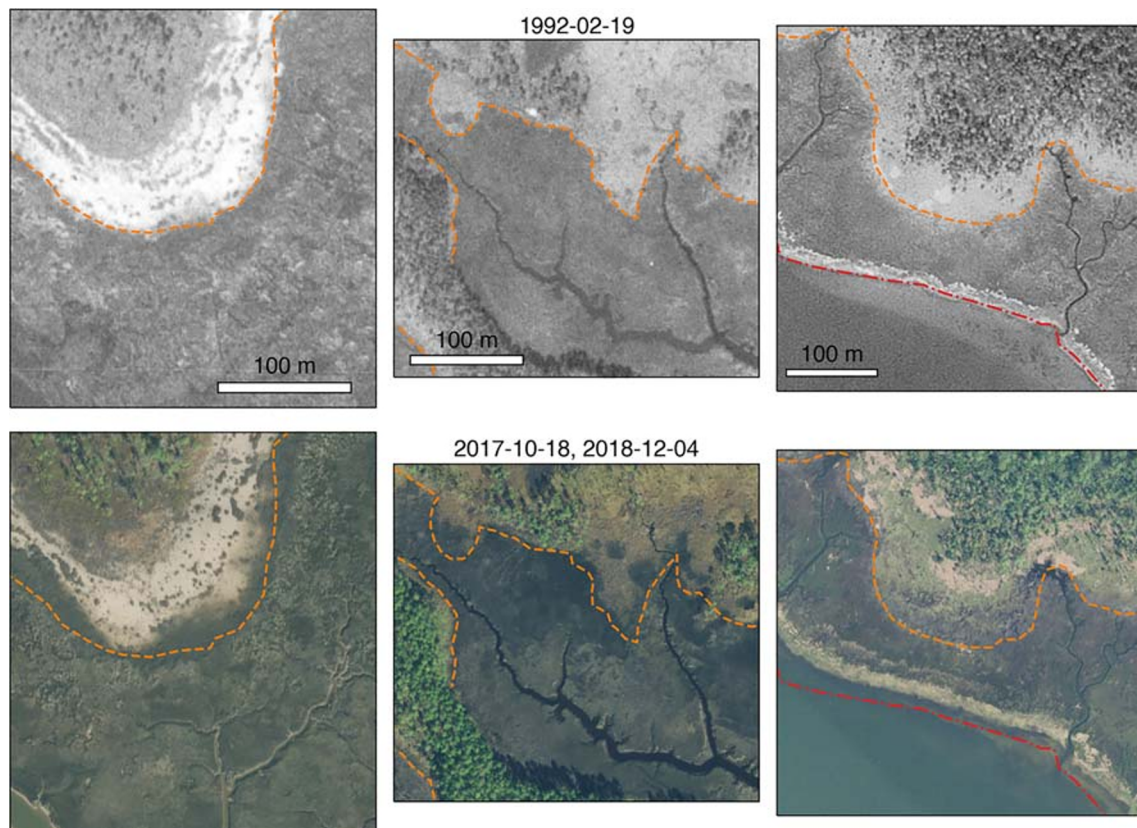
Fig. 10 Top row: aerial photos taken in 1992 (National Aerial Photography Program), and bottom row: photos from 2017/2018 (National Agriculture Imagery Program), at three locations (see Fig. 1) along the Grand Bay marsh–upland interface. The visually delineated 1992 marsh–upland boundary (dashed lines) and 1992 water–marsh boundary (dash-dotted lines; right column) show migration in the 2017/2018 photos

storms (including waves from routine storms as well as hurricanes) and sediment deficits conspire with sea-level rise to erode the shoreline and force marsh transgression.

Net Sediment Fluxes in the Context of Grand Bay's Geomorphic Trajectory

The net flux values computed in the "Net Sediment Fluxes" section can be compared to estimates of other relevant sedimentary processes in Grand Bay, including sea-level rise, vertical accretion, and erosion of the marsh edge.

Vertical Accretion Estimated from Sediment Fluxes

Local relative sea-level rise in the region is 4.31 ± 1.73 mm year^{-1}, based on an average of three nearby NOAA tide gauges (Fig. 1). By applying an appropriate sediment density and assuming all sediment imported via a channel is distributed evenly across its creekshed, equivalent sediment-accretion rates can be computed for the Heron Channel and Middle Channel creeksheds. Using a sediment density of 540 ± 240 kg m^{-3} (Morris et al. 2016; Marot et al. 2019) results in an inorganic accretion rate of 0.6 ± 0.3 mm year^{-1} for the sediment-import rate computed in the "Net Sediment Fluxes" section. In this context, sea-level rise is at least four times greater than the sedimentation rates estimated using our observational data. Because the majority of inorganic deposition likely occurs on or near the creek banks and organic deposition is dominant within the marsh interior, this value is likely an overestimate of the actual mineral deposition on the interior marsh (and perhaps an underestimate in the near-channel marsh). As a result, and despite the significant marsh-edge erosion occurring at points seaward, inorganic deposition does not appear sufficient to keep up with sea-level rise in this environment. Given the importance of organic-matter delivery via mud deposition (Mariotti et al. 2020), however, the combination of organic and inorganic deposition could help narrow the apparent gap between computed vertical accretion rates and sea-level rise.

Other Estimates Of Vertical Accretion

Other investigators have computed vertical sediment-accumulation rates in Grand Bay using geochemical and direct-measurement approaches. Darrow et al. (2017) estimated an accumulation rate of 2 mm year^{-1} using ^{210}Pb radiochronology, from a core taken near the mouth of Heron Channel, on the channel bed. Using surface-elevation tables (Cahoon et al. 2002), marsh-platform elevation-change rates of 2.5 ± 0.8 mm year^{-1} were computed at locations within the Middle Creek watershed (see Supporting Information). Both of these values are larger, by a factor of 3–4, than our instrument-derived estimates of sedimentation. The different time scales considered by the approaches could drive some of the variability in the estimates. Additionally, the SET approach includes accretion from organic material produced by vegetation, while our estimate is based solely on water-column delivery.

An equivalent vertical accretion rate can also be computed from observed lateral erosion rates. Given average rates of erosion over the past 150 year, approximately 6000 m^3 of material is delivered annually to Grand Bay between South Rigolets Island and Point aux Pins. Assuming equal delivery across the 20 km^2 of marsh plain surrounding Grand Bay results in an accretion rate of 0.3 mm year^{-1}. This value is far smaller than sea-level rise, but it neglects important spatial variability in observed sediment delivery and the potential for expansion at the landward marsh boundary. Nevertheless, the geochemical, SET, and erosion-rate estimates, in conjunction with those based on the sediment fluxes, suggest that vertical accretion on the marsh platform is less than local sea-level rise, which would ultimately lead to marsh drowning.

Sediment Fluxes Compared to Erosion Rates

At the scale of Middle Bay, an estimated 1800 t year^{-1} is eroded from the marshes surrounding the subembayment. The net import measured at MC, about 120 t year^{-1}, represents less than 10% of this eroded material. If Middle Bay marsh is assumed to be the sole sediment source for Middle Channel, then the remaining portion of the eroded marsh may settle on the seabed for later resuspension, or be transported to locations outside of Middle Bay and, potentially, outside of the Grand Bay system as a whole. By contrast, Fig. 6 suggests more than 200 times as much sediment is exported from Middle Bay as is imported to Middle Channel. In this context, relying on local Middle Bay erosion alone is insufficient to enable the magnitude of seaward flux computed at MB. This suggests the bay-width extrapolation as a potential source of error at the bay sites, additional sediment delivery from marsh erosion in nearby subembayments, or a deepening of the embayment from bed

erosion. Additionally, the 6 months of data presented here may not fully capture typical annual conditions of Grand Bay. Finally, the dynamics of the channelized and relatively wide marshes near the instrumented locations may differ from the narrower and less-channelized marshes on the east side of Grand Bay (Fig. 1).

SSC Increase from Marsh Erosion

With assumptions for eroded-sediment delivery, bay volume, and bay residence time, we can estimate an equivalent bay SSC increase that results from Middle Bay marsh erosion. In estimating delivery from marsh erosion E_m, we use lateral erosion rates of 0.5–3 m year^{-1}, marsh-platform heights of 0.2–0.6 m, marsh densities of 540 ± 240 kg m^{-3}, and a marsh-perimeter distance of 5000–6000 m. For bay volume V_b, we use bay surface areas of 1.5–2.5 km and mean depths of 0.75–1.5 m. We apply residence times T_R ranging from 1 to 8 days.

The SSC increase is then $E_m T_R / V_b$. Using these assumptions, 95% of the SSC-increase values fall between 0.5–71 mg L^{-1}, with a median value of 4.6 mg L^{-1}. Given that the average SSC at MB is 32 mg L^{-1} (median 24 mg L^{-1}; 95% of values 8–101 mg L^{-1}), the median marsh-derived value corresponds to about an 18% increase in SSC. Sea-breeze or event-scale dynamics will lead to greater increases in SSC than the median value computed using the long-term rates above. The strong temporal variability in marsh-derived SSC suggests that the use of a single SSC value as, for example, input to a marsh evolution model, may not be appropriate in environments like Grand Bay.

Comparison to Indicators of Marsh Stability

A conceptual understanding of the dynamics within Grand Bay enables us to place it within other models that use sediment fluxes as an indicator for wetland stability. Ganju et al. (2013) proposed an approach which accounts for the location of a wetland's dominant sediment source, its proximity to the wetland, and the mechanisms and timescales of sediment-source mobilization and transport. Grand Bay lacks relevant external sediment sources and relies on an internal sediment source—the marsh itself. Accordingly, this sediment is well within a single tidal excursion of the marsh and the channels that could advect it landward. Material is mobilized on diurnal to subtidal time scales by wind waves and is advected at the seiche, tidal, and subtidal time scales within channels. In this sense, it most resembles the Blackwater complex described in Ganju et al. (2013), although with important differences. The Blackwater system is also losing marsh from lateral wave erosion in a rapidly expanding internal open-water area, but tidal channels serve primarily to export sediment

at the subtidal timescale. Because the erosion in Grand Bay occurs seaward of the marsh instead of internally, channels are able to make use of that sediment via landward fluxes, albeit at a rate apparently insufficient to keep pace with sea-level rise.

Despite massive lateral wetland loss within Grand Bay, the intact marsh is relatively healthy. The unvegetated–vegetated marsh ratio is approximately 0.1, with minimal decadal change (Wasson et al. 2019), indicating marsh stability with little deterioration (Ganju et al. 2017). If the channel-as-importer role continues under higher sea levels, deposition rates increase to values greater than estimated in the "Vertical Accretion Estimated from Sediment Fluxes" and "Other Estimates Of Vertical Accretion" sections, and the marsh–upland boundary continues to migrate landward, Grand Bay may be able to transgress successfully as wave erosion continues to consume the marsh edge.

Conclusions

Oceanographic measurements, longer-term geochemical and surface-elevation observations, and numerical modeling results elucidate the complex geomorphic transition currently occurring over multiple timescales within Grand Bay. Our observations describe a divergent sedimentary system without a significant external sediment source that is influenced by diurnal and storm-event winds which erode the marsh edge and resuspend sediment. An increase in wave energy over the past 70 years following the loss of the subaerial Grand Batture islands has increased the lateral erosion rate, leading to a self-cannibalizing bay–marsh complex. Some of the water-column suspended material is transported landward in channels on subtidal and seiche time-scales. This material helps accomplish the process of marsh transgression as the seaward edge of the marsh is lost to wave attack and rising sea levels, and the marsh–upland interface migrates landward. The remainder of the material, and likely majority of the total, is exported to seaward locations via tidal and wind-driven fluxes. Quantifying these processes over a range of time scales and with a variety of methods helps determine the response of coupled bay–marsh systems to external sediment availability, edge erosion, and sea-level rise.

Compliance with Ethical Standards

References

Allen, J. 2000. Morphodynamics of Holocene salt marshes: a review sketch from the Atlantic and Southern North Sea coasts of Europe. *Quaternary Science Reviews* 19(12): 1155–1231. https://doi.org/10.1016/S0277-3791(99)00034-7.

Allen, J., and K. Pye. 1992. Coastal saltmarshes: their nature and importance. In: Saltmarshes: Morphodynamics, conservation and engineering significance. Cambridge: Cambridge University Press.

Basterretxea, G., A. Jordi, E. Garcés, S. Anglès, and A. Reñé. 2011. Seiches stimulate transient biogeochemical changes in a microtidal coastal ecosystem. *Marine Ecology Progress Series* 423: 15–28. https://doi.org/10.3354/meps08949.

Booij, N., R.C. Ris, and L.H. Holthuijsen. 1999. A third-generation wave model for coastal regions: 1. Model description and validation. *Journal of Geophysical Research* 104(C4): 7649–7666. https://doi.org/10.1029/98JC02622.

Cahoon, D.R., J.C. Lynch, B.C. Perez, B. Segura, R.D. Holland, C. Stelly, G. Stephenson, and P. Hensel. 2002. High-precision measurements of wetland sediment elevation: II. The rod surface elevation table. *Journal of Sedimentary Research* 72(5): 734–739. https://doi.org/10.1306/020702720734.

Csanady, G. 1973. Wind-induced barotropic motions in long lakes. *Journal of Physical Oceanography* 3: 429–438.

Darrow, E.S., R.H. Carmichael, K.R. Calci, and W. Burkhardt. 2017. Land-use related changes to sedimentary organic matter in tidal creeks of the northern Gulf of Mexico. *Limnology and Oceanography* 62(2): 686–705. https://doi.org/10.1002/lno.10453.

Davies, D.J., and R.L. Hummell. 1994. Lithofacies evolution from transgressive to highstand systems tracts, Holocene of the Alabama coastal zone. *Gulf Coast Association of Geological Societies Transactions* 44: 145–153.

Defne, Z., A.L. Aretxabaleta, N.K. Ganju, T.S. Kalra, D.K. Jones, and K.E. Smith. 2020. A geospatially resolved wetland vulnerability index: synthesis of physical drivers. *PLoS ONE* 15(1): 1–27. https://doi.org/10.1371/journal.pone.0228504.

DeWitt, N.T., C.A. Stalk, C.G. Smith, S.D. Locker, J.J. Fredericks, T.A. McCloskey, and C.J. Wheaton. 2017. Single-beam bathymetry data collected in 2015 from Grand Bay, Alabama-Mississippi. Tech. rep., U.S. Geological Survey Data Series 1070. https://doi.org/10.3133/ds1070.

Dyer, K. 1974. The salt balance in stratified estuaries. *Estuarine and Coastal Marine Science* 2(3): 273–281. https://doi.org/10.1016/0302-3524(74)90017-6.

Eleuterius, C.K., and G.A. Criss. 1991. Point aux Chenes: past, present and future perspective of erosion. Tech. rep., Physical Oceanography Section Gulf Coast Research Laboratory.

Eleuterius, L.N. 1976. The distribution of Juncus roemerianus in the salt marshes of North America. *Chesapeake Science* 17(4): 289–292. https://doi.org/10.2307/1350516.

Ennis, B., M.S. Peterson, and T.P. Strange. 2013. Modeling of inundation characteristics of a microtidal saltmarsh, Grand Bay National Estuarine Research Reserve, Mississippi. *Journal of Coastal Research* 30(3): 635. https://doi.org/10.2112/jcoastres-d-13-00041.1.

Fagherazzi, S. 2013. The ephemeral life of a salt marsh. *Geology* 41(8): 943–944. https://doi.org/10.1130/focus082013.1.

Fagherazzi, S., M.L. Kirwan, S.M. Mudd, G.R. Guntenspergen, S. Temmerman, A. D'Alpaos, J. van de Koppel, J.M. Rybczyk, E. Reyes, C. Craft, and J. Clough. 2012. Numerical models of salt marsh evolution: ecological, geomorphic, and climatic factors. *Reviews of Geophysics* 50(1): RG1002. https://doi.org/10.1029/2011RG000359.

Fagherazzi, S., G. Mariotti, P.L. Wiberg, and K.J. McGlathery. 2013. Marsh collapse does not require sea level rise. *Oceanography* 26(3): 70–77. https://doi.org/10.5670/oceanog.2013.47.

FitzGerald, D., I. Buynevich, and B. Argow. 2004. Model of tidal inlet and barrier island dynamics in a regime of accelerated sea level rise. *Journal of Coastal Research* SI(39): 789–795.

Friedrichs, C., and J. Perry. 2001. Tidal salt marsh morphodynamics: a synthesis. *Journal of Coastal Research* SI(27): 7–37.

Ganju, N.K., N.J. Nidzieko, and M.L. Kirwan. 2013. Inferring tidal wetland stability from channel sediment fluxes: observations and a conceptual model. *Journal of Geophysical Research:, Earth Surface* 118(4): 2045–2058. https://doi.org/10.1002/jgrf.20143.

Ganju, N.K., Z. Defne, M.L. Kirwan, S. Fagherazzi, A. D'Alpaos, and L. Carniello. 2017. Spatially integrative metrics reveal hidden vulnerability of microtidal salt marshes. *Nature Communications* 8. https://doi.org/10.1038/ncomms14156.

Gill, A.E. 1982. *Atmosphere–ocean dynamics*. San Diego: Academic Press.

Heimann, D.C., L.A. Sprague, and D.W. Blevins. 2011. Trends in Suspended-sediment loads and concentrations in the Mississippi River basin 1950–2009. Tech. rep., U.S. Geological Survey.

Hilbert, K.W. 2006. Land cover change within the Grand Bay National Estuarine Research Reserve. *Journal of Coastal Research* 226: 1552–1557. https://doi.org/10.2112/05-0582.1.

Leonardi, N., N.K. Ganju, and S. Fagherazzi. 2016. A linear relationship between wave power and erosion determines salt-marsh resilience to violent storms and hurricanes. *Proceedings of the National Academy of Sciences* 113(1): 64–68. https://doi.org/10.1073/pnas.1510095112.

Leonardi, N., I. Carnacina, C. Donatelli, N.K. Ganju, A.J. Plater, M. Schuerch, and S. Temmerman. 2018. Dynamic interactions between coastal storms and salt marshes: a review. *Geomorphology* 301: 92–107. https://doi.org/10.1016/j.geomorph.2017.11.001.

Luettich, R.A., S.D. Carr, J.V. Reynolds-Fleming, C.W. Fulcher, and J.E. McNinch. 2002. Semi-diurnal seiching in a shallow, micro-tidal lagoonal estuary. *Continental Shelf Research* 22(11-13): 1669–1681. https://doi.org/10.1016/S0278-4343(02)00031-6.

Marani, M., A. D'Alpaos, S. Lanzoni, and M. Santalucia. 2011. Understanding and predicting wave erosion of marsh edges. *Geophysical Research Letters* 38(21): 1–5. https://doi.org/10.1029/2011GL048995.

Mariotti, G., and J. Carr. 2014. Dual role of salt marsh retreat: long-term loss and short-term resilience. *Water Resources Research* 50: 2963–2974. https://doi.org/10.1002/2013WR014676.

Mariotti, G., T. Elsey-Quirk, G. Bruno, and K. Valentine. 2020. Mud-associated organic matter and its direct and indirect role in marsh organic matter accumulation and vertical accretion. *Limnology and Oceanography* 1–15. https://doi.org/10.1002/lno.11475.

Marot, M.E., C.G. Smith, T.A. McCloskey, S.D. Locker, N.S. Khan, and K.E. Smith. 2019. Sedimentary data from Grand Bay. Alabama/Mississippi, 2014–2016 (ver. 1.1 April 2020). https://doi.org/10.5066/P9FO8R3Y.

Meyer-Arendt, K.J., and K.A. Kramer. 1991. Deterioration and restoration of the Grande Batture Islands, Mississippi. *Mississippi Geology* 11(4): 1–5.

Mississippi Department of Marine Resources. 1999. Mississippi's Coastal Wetlands. Tech. rep. Mississippi Department of Marine Resources, Biloxi, MS.

Morris, J.T., D.C. Barber, J.C. Callaway, R. Chambers, S.C. Hagen, C.S. Hopkinson, B.J. Johnson, P. Megonigal, S.C. Neubauer, T. Troxler, and C. Wigand. 2016. Contributions of organic and inorganic matter to sediment volume and accretion in tidal wetlands at steady state. *Earth's Future* 4(4): 110–121. https://doi.org/10.1002/2015EF000334.

Myrick, R.M., and L.B. Leopold. 1963. Hydraulic geometry of a small tidal estuary. Professional Paper 422-B U.S. Geological Survey. https://doi.org/ 10.3133/pp422B.

Nowacki, D., N. Ganju, S. Suttles, J. Borden, and A. Nichols. 2018a. Discharge measurements made in Bayou Heron and Bayou Middle, Grand Bay, Mississippi in January 2017. https://doi.org/10.5066/P98NHB82.

Nowacki, D., S. Suttles, N. Ganju, E. Montgomery, and M. Martini. 2017. Oceanographic and water quality measurements collected in Grand Bay, Alabama/Mississippi, August 2016–January 2017. https://doi.org/10.5066/P9UG9JYQ.

Nowacki, D.J., and N.K. Ganju. 2019. Simple metrics predict Salt-Marsh sediment fluxes. *Geophysical Research Letters* 46(21): 12,250–12,257. https://doi.org/10.1029/2019GL083819.

Passeri, D.L., S.C. Hagen, S.C. Medeiros, and M.V. Bilskie. 2015. Impacts of historic morphology and sea level rise on tidal hydro-dynamics in a microtidal estuary (Grand Bay, Mississippi). *Continental Shelf Research* 111: 150–158. https://doi.org/10.1016/j.csr.2015.08.001.

Pestrong, R. 1965. The development of drainage patterns on tidal marshes (Vol. 10, 1–87). Palo Alto: Stanford University Publications.

Reed, D.J. 1989. Patterns of sediment deposition in subsiding coastal salt marshes, Terrebonne Bay, Louisiana: the role of winter storms. *Estuaries* 12(4): 222–227. https://doi.org/10.2307/1351901.

Rosencranz, J.A., N.K. Ganju, R.F. Ambrose, S.M. Brosnahan, P.J. Dickhudt, G.R. Guntenspergen, G.M. MacDonald, J.Y. Takekawa, and K.M. Thorne. 2016. Balanced sediment fluxes in southern California's Mediterranean-climate zone salt marshes. *Estuaries and Coasts* 39(4): 1035–1049. https://doi.org/10.1007/s12237-015-0056-y.

Ruhl, C.A., and M.R. Simpson. 2005. Computation of discharge using the index-velocity method in tidally affected areas. Scientific Investigations Report 2005-5004 U.S. Geological Survey. https://doi.org/10.3133/sir20055004.

Schieder, N.W., D.C. Walters, and M.L. Kirwan. 2018. Massive upland to wetland conversion compensated for historical marsh loss in chesapeake bay, USA. *Estuaries and Coasts* 41(4): 940–951. https://doi.org/10.1007/s12237-017-0336-9.

Siegel, A.F. 1982. Robust regression using repeated medians. *Biometrika* 69(1): 242–244. https://doi.org/10.2307/2335877.

Signell, R.P., R.C. Beardsley, H.C. Graber, and A. Capotondi. 1990. Effect of wave-current interaction on wind-driven circulation in narrow, shallow embayments. *Journal of Geophysical Research* 95(C6): 9671. https://doi.org/10.1029/jc095ic06p09671.

Smith, K., J. Terrano, N. Khan, and C. Stalk. 2020. Shore proximal sediment deposition, elevation, turbidity, and water level data for four sites in the coastal marsh at Grand Bay National Estuarine Research Reserve, Mississippi, from October 2016 through October 2017. https://doi.org/10.5066/P9BFR2US.

Stone, G.W., and R.A. McBride. 1998. Louisiana Barrier Islands and their importance in wetland protection: forecasting shoreline change and subsequent response of wave climate. *Journal of Coastal Research* 14(3): 900–915.

Suttles, S., D. Nowacki, N. Ganju, J. Borden, and A. Nichols. 2019. Suspended-sediment concentration data from water samples collected in 2016-17 in Grand Bay, Alabama and Mississippi. https://doi.org/10.5066/P91L4A75.

Terrano, J.F., K.E. Smith, J. Pitchford, J. McIlwain, and M. Archer. 2019. Shoreline change analysis for the Grand Bay National Estuarine Research Reserve, Mississippi Alabama:, 1848 to 2017. https://doi.org/10.5066/P9JMA8WK.

U.S. Geological Survey. 2017. Rapid salt-marsh erosion in Grand Bay, Mississippi. https://www.youtube.com/watch?v=S6TGEmu9dcA.

Wacker, K.P., and G.A. Criss. 1996. Erosional rates in the Point aux Chenes Bay area, Mississippi: 1990-1995. In: Sixtieth annual meeting of the Mississippi Academy of Sciences, 1–13.

Wasson, K., N.K. Ganju, Z. Defne, C. Endris, T. Elsey-Quirk, K.M. Thorne, C.M. Freeman, G. Guntenspergen, D.J. Nowacki, and K.B. Raposa. 2019. Understanding tidal marsh trajectories: evaluation of multiple indicators of marsh persistence. *Environmental Research Letters* 14(12): 124,073. https://doi.org/10.1088/1748-9326/ab5a94.

Wessel, P., and W.H.F. Smith. 1996. A global, self-consistent, hierarchical, high-resolution shoreline database. *Journal of Geophysical Research:, Solid Earth* 101(B4): 8741–8743. https://doi.org/10.1029/96JB00104.

Wilson, C.A., and M.A. Allison. 2008. An equilibrium profile model for retreating marsh shorelines in southeast Louisiana. *Estuarine, Coastal and Shelf Science* 80(4): 483–494. https://doi.org/10.1016/j.ecss.2008.09.004.

Wong, K.C. 1994. On the nature of transverse variability in a coastal plain estuary. *Journal of Geophysical Research* 99(C7). https://doi.org/10.1029/94JC00861.

Wright, L., and C. Nittrouer. 1995. Dispersal of river sediments in coastal seas: six contrasting cases. *Estuaries* 18(3): 494–508.

Zhang, X., N. Leonardi, C. Donatelli, and S. Fagherazzi. 2020. Divergence of sediment fluxes triggered by sea-level rise will reshape coastal bays. *Geophysical Research Letters* 47(13). https://doi.org/10.1029/2020gl087862.